Molecular Cell, Volume *53*

Supplemental Information

Structural Asymmetry in the Closed State of Mitochondrial Hsp90 (TRAP1) Supports a Two-Step ATP Hydrolysis Mechanism

Laura A. Lavery, James R. Partridge, Theresa A. Ramelot, Daniel Elnatan, Michael A. Kennedy, and David A. Agard

Supplemental Information

Supplemental Figures and Legends

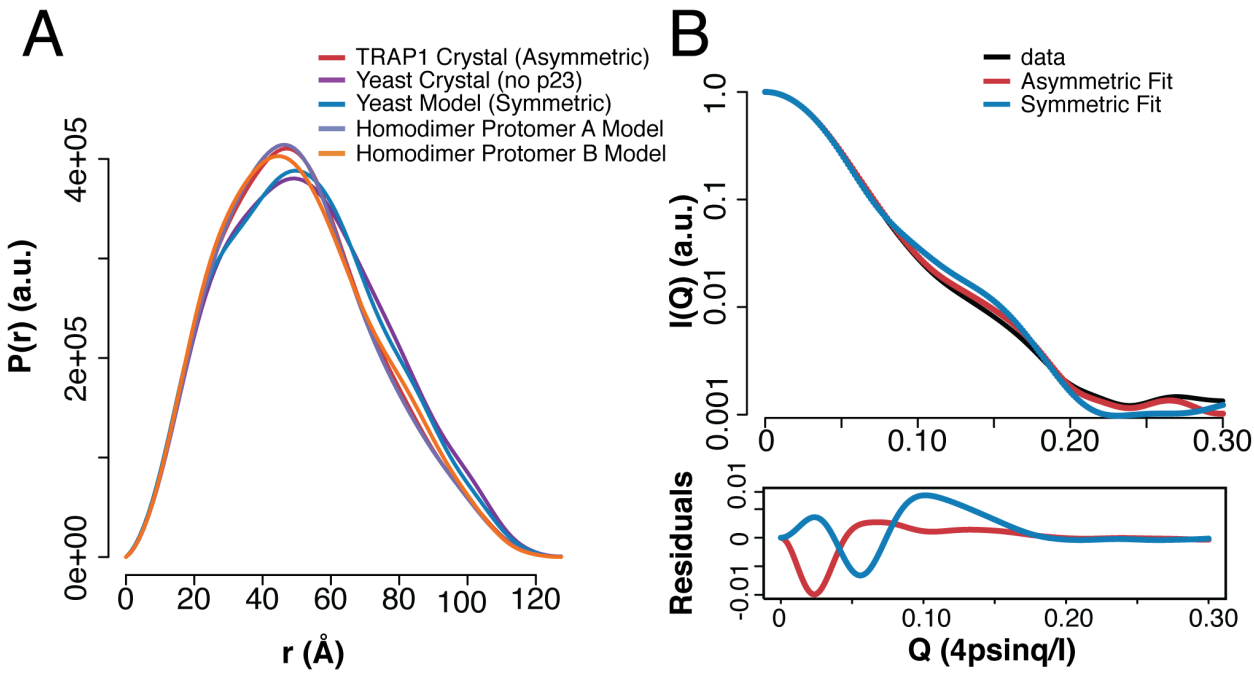

Figure S1. Theoretical SAXS curves for closed state models. (Related to Figure 4A/B) A) Scaled theoretical P(r) curves generated for a series of closed state models using CRYSOL (Svergun D.I., 1995) and GNOM (Svergun, 1992). Here we see differences in the inter-atomic distance distributions for each model. These curves were used for further fitting and assessment of the closed state conformation in solution. B) Representative averaged and scaled scattering data (black) fit as in Figure 4B demonstrating the asymmetric crystal structure is a better fit to the solution conformation of TRAP1. Data is hTRAP1 closed with AMPPNP.

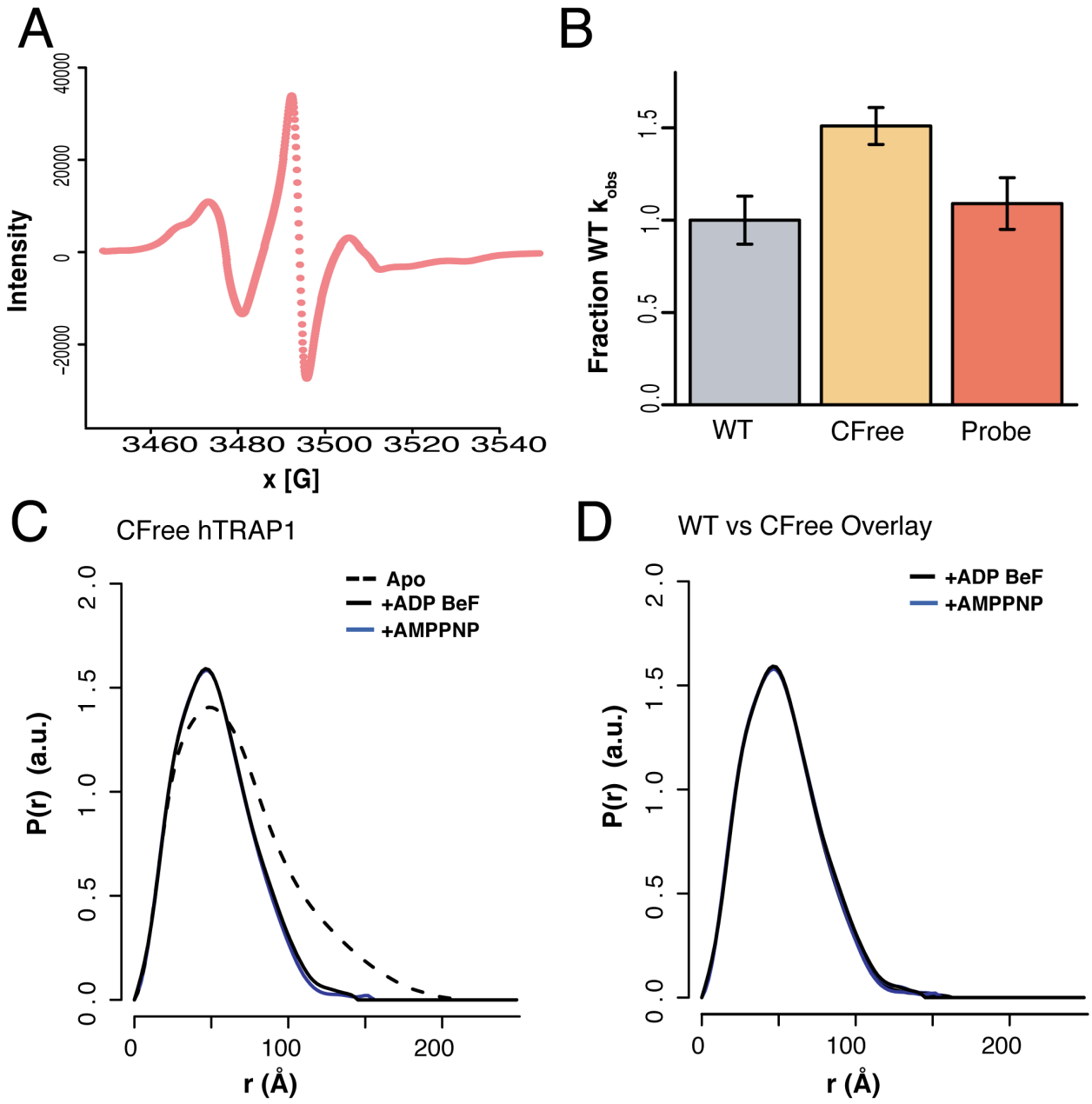

Figure S2. DEER probe is labeled, active and forms an asymmetric closed state. (Related to Figure 4C/D) A) Continuous-wave (CW) EPR confirming site-specific labeling of the MSL spin probe. B) ATPase measurements of wild-type (WT), cysteine-free (CFree), and probe used in DEER measurements (Probe) in figure 4D. (Error bars are propagated standard deviations) C) SAXS measurements for CFree human TRAP1 showing a characteristic shift with addition of ATP analogs. D) Overlay of SAXS curves of WT and CFree hTRAP1 illustrating excellent conservation of overall closed state conformation.

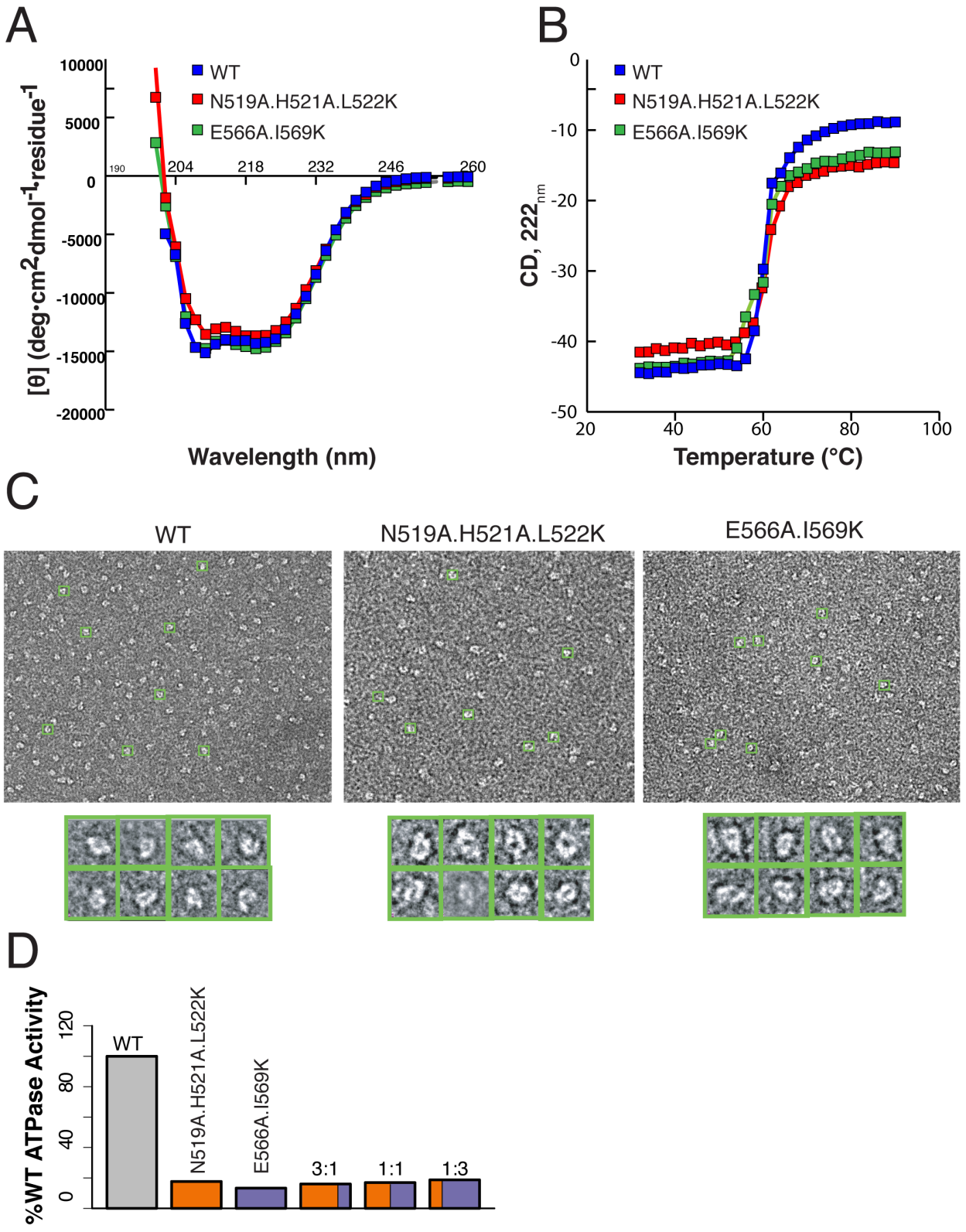

Figure S3. Characterization of MD:CTD Interface mutations. (Related to Figure 5) A) Circular dichroism (CD) spectra and B) melting curves of apo WT and the two most severe mutants from zebrafish TRAP1 (zTRAP1) (N519A.H521A.L522K, E566A.I569K)

aimed at disrupting the unique MD:CTD interfaces of protomer A and protomer B, respectively. These data demonstrate that overall secondary structure and stability are not significantly altered upon mutation. C) Negative stain EM micrographs of pre-closed WT and mutants used in A/B. Particles representing a closed form of the chaperone are shown below their respective micrographs. D) ATPase measurements using a previously reported radioactive assay (see Extended Experimental Procedures) of WT and point mutations from A/B. Mixing in different ratios allows the contributions of the heterodimer to be separated from those of the two homodimers also present in solution (see Cunningham et al, JBC 2008). No change of activity is observed by mixing the most severe MD:CTD mutants suggesting that proper progression through the ATP cycle requires the ability to sample both conformations.

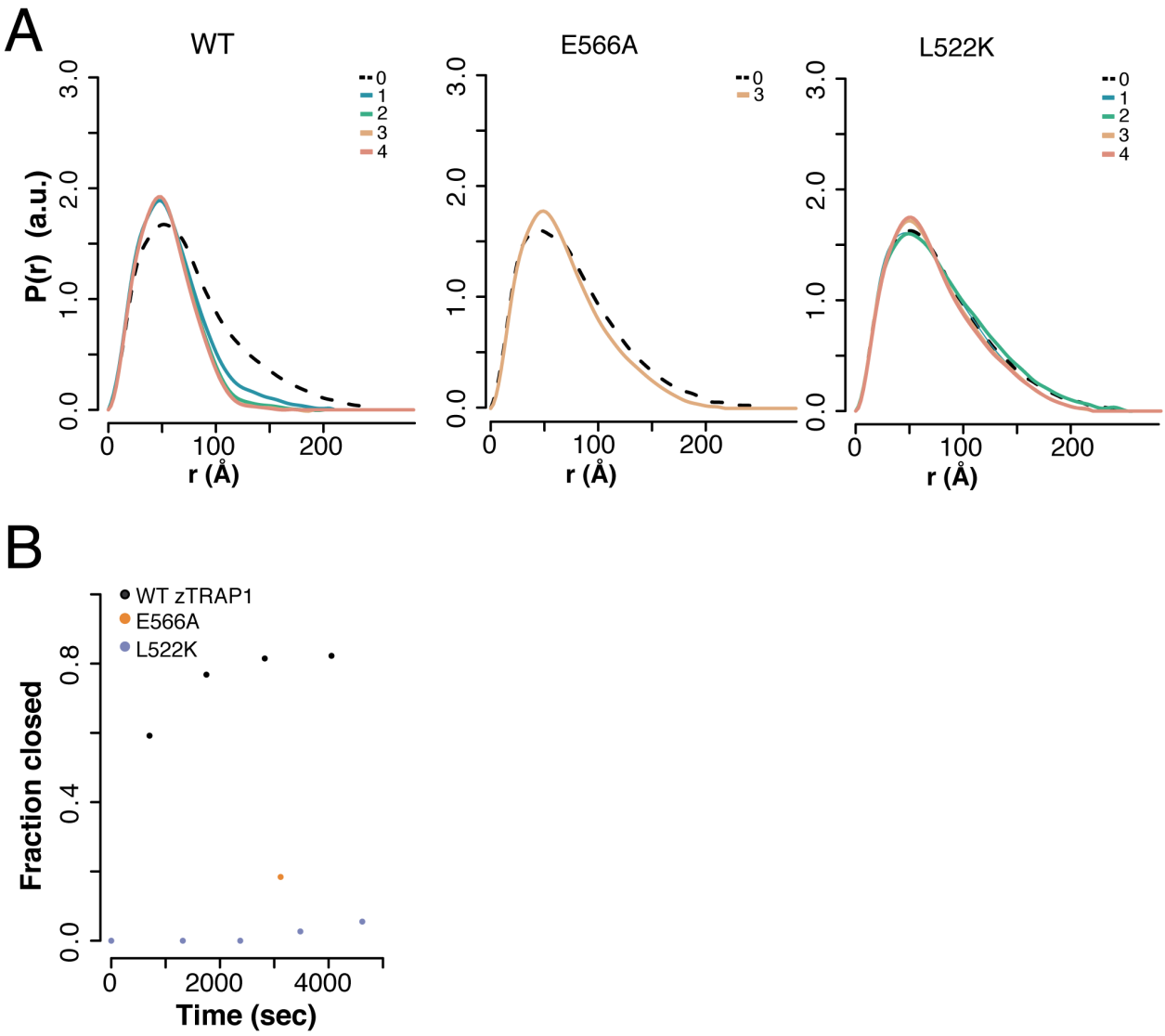

Figure S4. MD:CTD interface mutants destabilize the closed state. (Related to figure 5) A) SAXS curves of zTRAP1 in the apo state (0) and time points following

addition of ADP-BeF (1-4, corresponding to ~700,1000,1320… seconds, respectively). For WT, the addition of ADP-BeF shows initiation of closure reaction at time point 1 and continues to accumulate over time. Although the MD:CTD interface mutants (E566A Protomer B, L522K Protomer A) accumulate closed state molecules, the percent of the population at the later time points is significantly less than WT. B) Plotting the percent closed state over time (least squares fitting, see methods) demonstrates that the approach to a closed state equilibrium is much slower for both mutants.

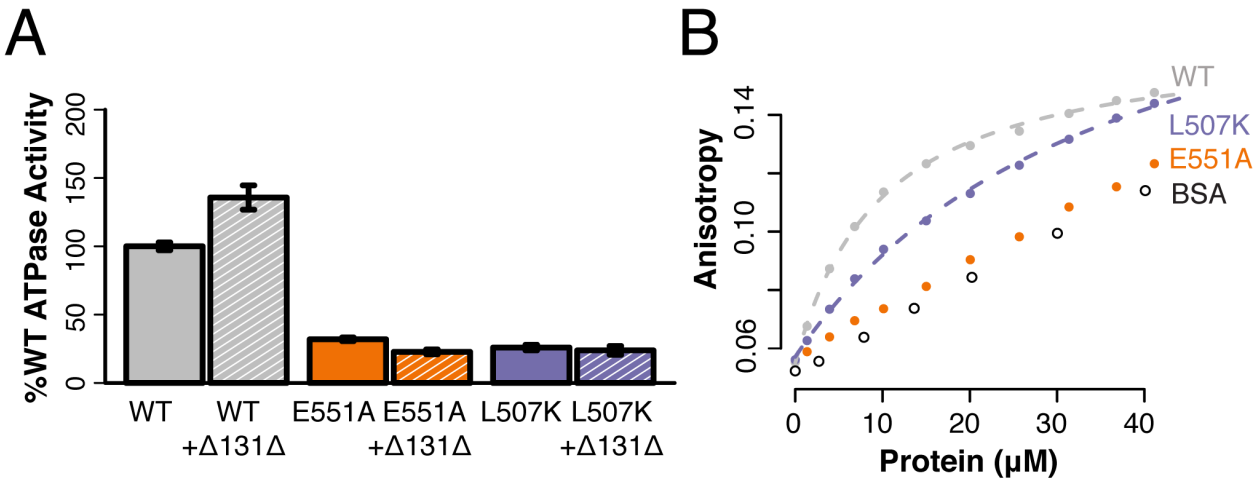

Figure S5. MD:CTD interface mutants have altered interaction with Δ131Δ. (Related to figure 5) A) Comparison of steady-state hydrolysis rates for WT hTRAP1 and MD:CTD mutants +/- Δ131Δ (model substrate). While Δ131Δ can stimulate the ATPase of WT hTRAP1 similar to bHsp90 (Street et al., 2011), in the presence of the MD:CTD interface mutants substrate acceleration is no longer observed. (Error bars are propagated standard deviation) B) Anisotropy binding assay with IAEDANS-labeled Δ131Δ demonstrating binding of WT hTRAP1 with a ~9μM Kd and a lower K_d (~35μM) for the MD:CTD interface mutant aimed to disrupt protomer A (L507K). Binding for the mutant aimed to disrupt the MD:CTD interface of protomer B (E551A) could not be detected above background (BSA). Negative stain EM showed that both WT and the E551A mutant were ~100% closed, while the L507K mutant was estimated to be ~30% closed (data not shown). Together these data suggest altered substrate interaction in the closed state of TRAP1 due to changes in conformation of the asymmetric MD:CTD interfaces upon mutation.

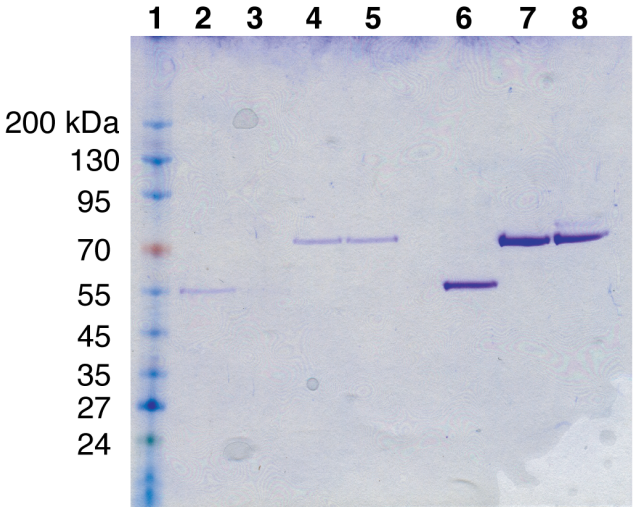

Well #	
1	NEB ColorPlus Protein Ladder
2	E566A.I569K Crystal#1
3	E566A.I569K Crystal#2
4	WT Crystal#1
5	WT Crystal#2
6	500ng NTD:MD Fragment stock
7	500ng E566A.I569K stock
8	500ng WT stock

Figure S6. NTD:MD crystal is formed after cleavage of full-length TRAP1 at a destabilized MD:CTD interface. (Related to Figure 6) Coomassie stained gel of stock protein and representative WT and mutant crystals that led to the structures presented in Figures 1 and 6, respectively. Pre- and post-crystallization the WT protein remains full-length. The crystallized mutant protein has been cleaved between the Middle and C-Terminal domains leading to a NTD:MD dimer while keeping the catalytic machinery seemingly intact (Figure 4).

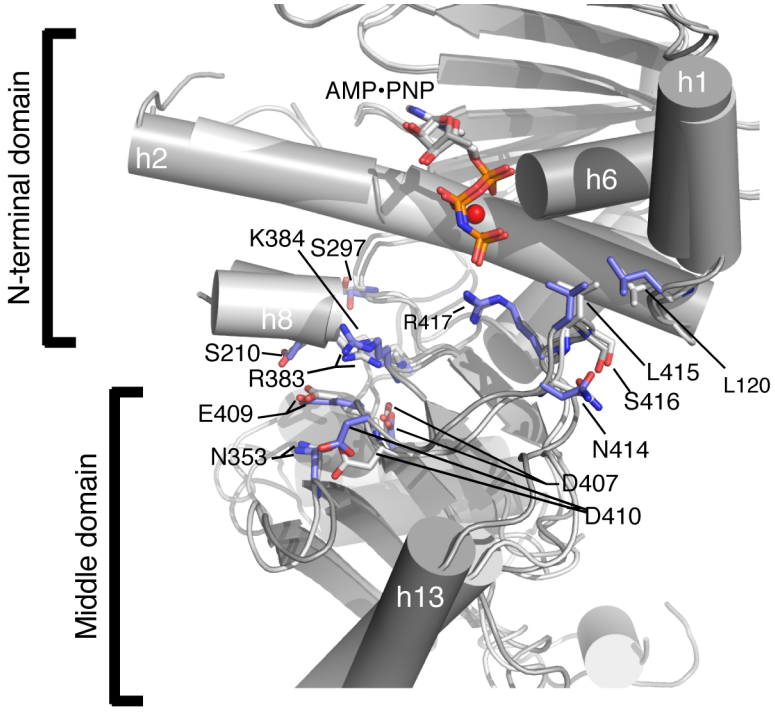

Figure S7. NTD alignment of Full-length and NTD:MD TRAP1. (Related to Figure 6) NTD alignment of the full-length and NTD:MD TRAP1 structures with a view of the NTD and LMD interface similar to Figure 3C. Selected side-chains from protomer A of full-length and NTD:MD structure are colored slate and grey, respectively. Although the catalytic machinery remains more or less intact, structural deviations start to become apparent past R417.

Movie S1. Morph between the TRAP1 and yHsp90 conformations. (Related to Figure 1) Morph between the TRAP1 crystal structure and the yHsp90 crystal structure (a homodimer very similar to protomer B) clearly shows the dramatic conformational changes compatible with full-length closed Hsp90 structures. Residues corresponding to those that affect client binding in bHsp90 and yHsp90 (Genest et al., 2013) are highlighted in red, illustrating how they are differentially organized (separated in the A protomer, but clustered in the B protomer and the yHsp90). Morph made using UCSF Chimera Package (Pettersen et al., 2004).

Movie S2. Residues that bind with client protein change conformation between asymmetric states. (Related to Figure 3) Residues previously shown to bind client proteins (also highlighted in Movie S1) are colored red. A morph between the two protomers of the TRAP1 crystal structure clearly demonstrate the drastic conformational change at the MD:CTD interface that re-arranges the client interface.

Movie S3. Conformational morph of full-length TRAP1 to NTD:MD crystal structure. (Related to Figure 6) Morph (UCSF Chimera) of asymmetric conformation

seen in the full-length structure of TRAP1 to the symmetric NTD:MD structure. Here we see that cleavage of the CTD in the asymmetric closed state relieves strain at the MD:CTD interface resulting in slight shifts in the in NTD and NTD:LMD interface, as well as swinging out of the MDs. These shifts ultimately result in restoration of dimer symmetry.

Supplemental Tables

Table S1. R values for closed state model fitting of SAXS data

SAXS data	Model	R value
WT hTRAP1 ADP BeF	TRAP1 Crystal (Asymmetric)	**0.015**
WT hTRAP1 ADP BeF	Yeast Crystal (no p23)	0.072
WT hTRAP1 ADP BeF	Yeast Model (Symmetric)	0.064
WT hTRAP1 ADP BeF	Homodimer models A+B	0.021
WT hTRAP1 AMPPNP	TRAP1 Crystal (Asymmetric)	**0.016**
WT hTRAP1 AMPPNP	Yeast Crystal (no p23)	0.063
WT hTRAP1 AMPPNP	Yeast Model (Symmetric)	0.057
WT hTRAP1 AMPPNP	Homodimer models A + B	0.021
WT zTRAP1 ADP BeF	TRAP1 Crystal (Asymmetric)	**0.026**
WT zTRAP1 ADP BeF	Yeast Crystal (no p23)	0.057
WT zTRAP1 ADP BeF	Yeast Model (Symmetric)	0.05
WT zTRAP1 ADP BeF	Homodimer models A + B	0.031
WT zTRAP1 AMPPNP	TRAP1 Crystal (Asymmetric)	**0.030**
WT zTRAP1 AMPPNP	Yeast Crystal (no p23)	0.070
WT zTRAP1 AMPPNP	Yeast Model (Symmetric)	0.061
WT zTRAP1 AMPPNP	Homodimer models A + B	0.035
CFree hTRAP1 ADP BeF	TRAP1 Crystal (Asymmetric)	0.**015**
CFree hTRAP1 ADP BeF	Yeast Crystal (no p23)	0.063
CFree hTRAP1 ADP BeF	Yeast Model (Symmetric)	0.059
CFree hTRAP1 ADP BeF	Homodimer models A + B	0.016
CFree hTRAP1 AMPPNP	TRAP1 Crystal (Asymmetric)	**.017**
CFree hTRAP1 AMPPNP	Yeast Crystal (no p23)	.067
CFree hTRAP1 AMPPNP	Yeast Model (Symmetric)	.059
CFree hTRAP1 AMPPNP	Homodimer models A + B	0.020

Note: **Bold** represents the best fit. (Related to Figure 4)

Table S2. Steady-state kinetic values

TRAP1 Protein (WT or Mutant)	zTRAP1 Kobs (min-1)	hTRAP1 Kobs (min-1)
WT	1.21 +/- 0.07	0.32+/-.01
E/A.I/K	0.29 +/- 0.01	
N/A.H/A.L/K	0.22 +/- 0.01	
E/A	0.46+/- .02	0.10+/- .01
L/K	0.34 +/- .05	0.07+/- .01
L/S		0.16 +/- .01
V/A		.22+/- .02
Cysteine Free (CFree)		.67+/-0.03
WT Km (25 °C)		8.3 μM
WT Km (30 °C)	25.1 μM	8.5 μM

Note: Errors are standard deviations. (Related to Figure 5)

Extended Experimental Procedures

Protein Production and Purification

TRAP1 homolog purifications

We obtained the full-length TNF receptor-associated protein 1 (TRAP1) gene of *Homo sapiens* and *Danio rerio* from the mammalian and zebrafish gene collections (Invitrogen and Thermo Scientific, respectively). The mature sequences (residues 60-704 and 73-719 *H. sapiens* and *D. rerio*, respectively) of TRAP1 were cloned into the pET151/D-TOPO bacterial expression plasmid (Invitrogen), resulting in N-terminally His-tagged TRAP1 fusion proteins. Between the 6x-His-tag and TRAP1 is a TEV protease cleavage site. The resulting plasmid was transformed into *E. coli* BL21 (DE3)-RIL for protein expression.

For expression of TRAP1 from *D. rerio* (zTRAP1, WT and mutant forms), cells were grown at 30°C in Luria-Bertani broth supplemented with 0.4% glucose to OD600 = 0.8 and induced with 0.4 mM IPTG at 16°C for 18 hours. Cells were harvested by centrifugation, resuspended in 50 mM potassium phosphate pH 8.0, 500 mM NaCl, 20 mM imidazole, and 3 mM β-mercaptoethanol. Cells were lysed using an EmulsiFlex-C3 (Avestin). The crude lysate was immediately supplemented with 0.2 mM phenylmethylsulfonyl fluoride (PMSF) and centrifuged at 20,000 g for 20 minutes. The soluble fraction was subsequently incubated with 2 mL Ni-NTA (GE Healthcare) per 1,000 ODs for 1 hour at 4°C. Following incubation with the Ni-NTA resin, lysate was removed by pelleting resin at 2,500

g for 3 minutes and washed 3 times with 9 bed volumes of 50 mM potassium phosphate pH 8.0, 500 mM NaCl, 20 mM imidazole, and 3 mM β-mercaptoethanol. Following the batch wash Ni-NTA resin was loaded onto a gravity column and His-tagged protein was eluted with 6 bed volumes of 50 mM potassium phosphate pH 8.0, 300 mM NaCl, 500 mM imidazole, and 3 mM β-mercaptoethanol. Eluted protein was dialyzed overnight against 10 mM Tris/HCl pH 8.0, 200 mM NaCl, and 1 mM DTT and the 6x-His-tag was cleaved using a 20:1 molar ratio of protein:TEV protease. The protein was purified by anion exchange chromatography on a HiTrapQ or MonoQ 10/100 GL column (GE Healthcare) via a linear NaCl gradient and twice by size exclusion chromatography using a Superdex S200 26/60 column (GE Healthcare) run in 10 mM Tris/HCl pH 8.0, 100 mM NaCl, 1 mM DTT. Selenomethionine derivatized WT zTRAP1 was prepared by growing BL21 (DE3)-RIL cells in M9 Medium (Sigma) supplemented with 1 mM $MgSO_4$, 6.6 μM $CaCl_2$, 1 ml $FeSO_4$ (4.2 mg/ml), 0.4% glucose, and 100 μl 0.5% (w/v) thiamine at 37°C (modified from (Doublie, 1997)). At OD600 = 0.5 solid amino acid supplements were added (100 mg/ml L-lysine, L-phenylalanine, and L-threonine; 50 mg/ml L-isoleucine, L-leucine, L-valine, and L-selenomethionine). After 30 minutes, cultures were transferred to 22 °C for 20 minutes and then induced with 0.2 mM IPTG for 18 hours. The selenomethionine-derivatized protein was purified as described for the native version with a final buffer of 20 mM Hepes pH 7.5, 50 mM KCl, 2 mM $MgCl_2$, and 5 mM DTT. Incorporation of selenomethionine was confirmed by

mass spectrometry (data not shown). Both the native and selenomethionine derivative proteins were concentrated to ~25 mg/mL for crystallization and flash frozen for storage. TRAP1 from *H. sapiens* (hTRAP1, WT and mutant forms) were purified in a similar fashion to zTRAP1 proteins with a final buffer of 20 mM Hepes pH 7.5, 50 mM KCl, 2 mM $MgCl_2$, and 1 mM DTT.

Mutant forms for all homologs were made from the vector constructs described above using standard PCR methods.

Δ131Δ purification

WT and cysteine variant (D19C, (Gillespie and Shortle, 1997)) Δ131Δ were expressed in *E. coli* BL21 (DE3), grown in Terrific broth, and induced with 1mM IPTG at OD_{600} ~0.8 for 4 hours at 37 ˚C. Cells were pelleted and subsequently lysed by resuspension in buffer containing 6 M Urea, 25 mM Tris pH 8.0 and 2.5 mM EDTA (Buffer #1) and stirring for 30 min at 4 ^{o}C. Lysate was spun down at 10,000 g for 20 minutes using a Sorvall GSA rotor. Resulting inclusion body pellet was solubilized in Buffer #1 + 400 mM NaCl (+2 mM DTT for the cysteine variant) by stirring vigorously at 4 ˚C for 1 hr. The solubilized inclusion body is further clarified by centrifugation as done in the previous step. Equal volume of ice-cold EtOH was added to the supernatant and incubated for 1 hr for -20 ˚C to precipitate nucleic acids. After pelleting, an equal volume of ice-cold EtOH was added to the resulting supernatant and was incubated overnight at -20 ˚C.

Precipitated protein was dissolved in Buffer #1 and loaded onto SP-sepharose resin (GE Healthcare) equilibrated with the same buffer. Protein was refolded on the SP-sepharose column by washing with 2CV of 25 mM Tris pH 7.5, 25 mM KCl, 5 mM MgCl2, 2 mM DTT, and eluted with salt gradient from 150 mM – 800 mM KCl. Chosen fractions were dialyzed into a buffer containing 50 mM Hepes pH 7.5, 50 mM KCl, 5 mM MgCl2 (+2 mM DTT for cysteine variant), followed by size exclusion chromatography (S200 16/60) in the same buffer (+0.2 mM TCEP for cysteine variant in place of DTT).

The D19C variant was labeled with 5-molar excess of 5-({2-[(iodoacetyl)amino]ethyl}amino)naphthalene-1-sulfonic acid (IAEDANS) (Life Technologies) at room temperature for 3 hr. Unreacted dyes were removed via extensive dialysis.

Crystallography

WT zTRAP1 was screened for crystallization conditions at a concentration of 10 mg/mL and incubated in a crystallization buffer (20 mM Hepes 7.5, 50 mM KCl, and 2 mM $MgCl_2$, 2 mM AMPPNP or 2 mM ADP + 1X BeF_2 / AlF_3) for 30 minutes prior to crystallization. BeF_2 and AlF_3 were made by mixing 200 mM $BeCl_2$ / $AlCl_3$ and 1 M KF to make a 5X BeF_2 / AlF_3 solution of 10 mM $BeCl_2$ / $AlCl_3$ and 50 mM KF.

For screening we used a mosquito liquid handling robot (TTP Lab Tech) and three commercially available deep well screening blocks: JCSG+ and Protein Complex Suite (Qiagen) as well as the Index HT screen (Hampton Research).

The initial crystallization hit was refined to 18% (v/v) PEG3350 and 0.2 M sodium malonate pH 6.6 by the hanging drop vapor diffusion method at 23 °C. The additive screen HT (Hampton Research) was used to isolate hexammine cobalt (III) chloride as an additive that greatly improved crystal size and overall morphology. The final crystallization condition used was 18% (v/v) PEG3350, 0.2 M sodium malonate pH 6.6 - 7, 20 – 42 mM hexamine cobalt mixed 1:1 with TRAP1 protein at 7-10 mg/mL. Our optimized crystals grew in 7-10 days at 23 °C using the hanging drop vapor diffusion method forming 100 μm x 100 μm x 200 μm crystals. The selenomethionine derivative protein crystallized in a similar condition. Both native and derivative crystals were cryoprotected by adding glycerol (10-12% (v/v) final concentration) to the reservoir solution before flash-freezing in liquid nitrogen. Crystal screening and data collection were carried out at beamlines 8.3.1, 8.2.1, and 8.2.2 at the Advanced Light Source (ALS) and the final X-ray data was collected at beamline 8.3.1. The native and selenomethionine derivatized protein of TRAP1 were crystallized in the $C2_1$ spacegroup with one TRAP1 dimer per asymmetric unit (PDB codes: 4JOB, 4IYN, and 4IPE).

For the N-terminal:Middle domain (NTD:MD) crystal structure, full-length protein was purified and screened in a similar fashion (buffer condition at the time of screening was 20 mM Hepes pH7.5, 50 mM KCl, 2 mM $MgCl_2$, 1 mM DTT), using full-length zTRAP1 with a double point mutation at E556A.I569K. These mutations effectively destabilize the Middle-CTD (MD:CTD) interface present in

protomer B of the full length crystal structure. The initial crystallization hit was refined to a final condition of 5 mg/mL protein in a 1:1 ratio with 0.1 M Sodium Phosphate monobasic pH 6.5, and 12% PEG 8000. Our optimized crystals grew in 10-14 days at 23 °C using the hanging drop vapor diffusion method forming 100 μm x 100 μm x 200 μm crystals. Crystals were harvested and cryoprotected with 12% (v/v) glycerol prior to flash-freezing in liquid nitrogen. Data collection was carried out at the ALS at beamline 8.3.1. This data set could easily be scaled and merged in the I222 spacegroup containing a single TRAP1 protomer, already indicative of a high degree of symmetry between protomers. We chose to build and refine the structure in the $C2_1$ spacegroup, and similar to the full-length structure the spacegroup $C2_1$ contains two protomers to complete one dimerized biological unit. This symmetry persisted in $C2_1$ and we chose to build our final model in the I222 spacegroup, as we saw no significant differences between protomers in the ASU (PDB code: 4IVG).

Structure Determination

Data reduction was carried out using HKL2000 (Otwinowski and Minor, 1997). Structures of zTRAP1 bound to ADP-AlF_4 and ADP-BeF_3 were solved using the single-wavelength anomalous dispersion (SAD) method with selenomethionine derivatives. The positions of 36 selenium sites (out of 38 possible per zTRAP1-dimer) were found using AutoSol from the PHENIX program suite and used for subsequent phasing (Adams et al.). The selenium

positions and experimental map allowed us to clearly define domains of zTRAP1 that allowed us to build a full-length model. The final models for zTRAP1 bound to ADP-AlF_4 or ADP-BeF_3 were built with native data and refined to an extended resolution of 2.3 Å. The structure of zTRAP1 bound to AMPPNP was solved using molecular replacement and the zTRAP1 model bound to ADP-AlF_4. The final NTD:MD zTRAP1 structure bound to AMPPNP was solved with molecular replacement and a monomer of the full-length zTRAP1 model truncated at the MD:CTD interface. All models of TRAP1 were built using COOT (Emsley and Cowtan, 2004) and further refinement was carried out using the latest builds of the PHENIX suite (Adams et al.).

A majority of the secondary structural elements have been built with the exception of helix 5 (residues 132-136) of protomers B and helix 21 (residues 568-579) in the C-terminal domain of both protomers in the full-length structure. Some loops have been omitted due to poor electron density and very high B-factors. Figures were made using PyMOL (Schrödinger, 2010) and UCSF Chimera Package (Pettersen et al., 2004). Chimera is developed by the Resource for Biocomputing, Visualization, and Informatics at the University of California, San Francisco (supported by NIGMS 9P41GM103311).

Structural Comparisons

In Figure 3 the four major domains of TRAP1-AMPPNP were individually aligned using monomer A and monomer B and the "*match"* command in Chimera

to obtain RMSD values for every residue. These RMSD values were then imported into the B-factor column of monomer B from the TRAP1-AMPPNP structure. The “cartoon putty” feature of PyMOL was used to represent increasing RMSD values as thicker tubes with a transition in color from blue to yellow.

Steady-state Hydrolysis Measurements

Protein concentration was calculated using the Edelhauc method (Gill and von Hippel, 1989). Steady-state hydrolysis rates were measured using the previously described ATP regenerating assay (Leskovar et al., 2008) on an Agilent 8453 dioade array. Assay components were mixed to a final concentration of 200 μM NADH, 400 μM PEP, 50 U/mL PK, 50 U/mL LDH, at least 10-fold excess ATP over the measured K_m (Table S2), and in a final buffer of 40 mM Hepes pH 7.5, 150 mM KCl, 5 mM $MgCl_2$. For ATPases with the model substrate, 10 µM hTRAP1 was incubated +/- 15 µM WT Δ131Δ in buffer conditions matching anisotropy binding described below. Background change in NADH absorbance (340 nm) was monitored to ensure a flat baseline before addition of 5 μM (or 10 µM) chaperone (monomer concentration). The change in NADH absorbance after protein addition was monitored and slope obtained by subtracting baseline at 750 nm followed by least squares fitting to a simple linear regression model. K_{obs} values were calculated using the equation below:

k_{obs}= |slope/(E_{nadh}*c)|

where k_{obs} is the observed rate of hydrolysis (s^{-1}), E_{nadh} is the extinction coefficient of NADH (6220 $M^{-1}s^{-1}$), and c is the monomer protein concentration (M). For bar plots the rates were normalized by the WT rate and standard deviations were error propagated via standard equations.

For MD:CTD interface mutant mixing experiment (Figure S3D), we used a previously reported radioactive assay (Cunningham et al., 2008), with 2uM protein (monomer), 650 μM ATP at 37 ^{o}C in a buffer containing of 20 mM Hepes pH 7.5, 50 mM KCl, 2 mM $MgCl_2$, and 1 mM DTT. Prior to initiating the reaction with ATP, heterodimers were formed under apo conditions at 30 ^{o}C for 30 minutes.

All homologs were inhibited with the Hsp90 specific inhibitors (Radicicol, data not shown) and results were plotted using the program R (R Development Core Team, 2010).

Negative Stain Electron Microscopy

WT zTRAP1, zTRAP1 E566A.I569K and zTRAP1 N519A.H521A.L522K were initially diluted to .1 mg/mL in a buffer containing 20 mM Hepes 7.5, 50 mM KCl, and 2 mM $MgCl_2$, + 2 mM ADP-BeF_3 (BeF prepared as above). Reactions were incubated at RT for 30 minutes, followed by dilution to 0.01 mg/mL in the buffer above including ADP-BeF_3. 5 μL of the resulting reactions were then incubated for ~1 minute on 400 mesh Cu grids (Pelco). Grids were previously

coated with Collodion (EMS) and then coated with a thin carbon layer (~100 Å). Following sample incubation was a 3X wash with miliQ water, and lastly stained 3X with uranyl formate, pH 6. The last stain was removed by vacuum until the surface of the grid was dry. Prepared grids were imaged with a TECNAI 20 (FEI) operated at 120 kV. Images were recorded using a 4k x 4k CCD camera (Gatan) at 62,000 x magnification, at -1.5 μm defocus (1.8Å/pix). Representative closed state particles (Figure S3C) were selected in EMAN (Ludtke et al., 1999).

Circular Dichroism Spectroscopy

zTRAP1 E566A.I569K and zTRAP1 N519A.H521A.L522K were buffer exchanged with size exclusion chromatography into a 5 mM Hepes/NaOH pH 7.4 and 150 mM NaCl buffer immediately prior to the experiment. An Aviv Model 202 CD spectrometer was used for all experiments. CD signal at 220 nm of 0.5 mg/mL protein in a 1 mm path length cell was recorded at every degree during a 25-80 °C temperature ramp with two minutes of equilibration time at each step. Raw CD data was converted to units of mean residue elipticity [θ] (degrees cm^2 $dmol^{-1}$ $residue^{-1}$).

SAXS Reaction, Data Collection and Analysis

WT TRAP1 homologs and mutant proteins were buffer exchanged into 20 mM Hepes pH 7.5, 50 mM KCl, 2 mM $MgCl_2$, 1mM DTT immediately prior to the experiment. 75 μM protein (monomer) was used as the final concentration for all

reactions. In the reactions where ADP-BeF_3 was used as the nucleotide analog, 1X BeF was made as described in the crystallography methods section above and added to both reactions to allow for direct comparison. 2 mM nucleotides were used to initiate closure and the reactions were incubated at 30 °C for 10 hours. Reactions were spun down at max speed in a tabletop centrifuge for 10 minutes immediately prior to data collection to remove any trace aggregation.

For time course experiments, zTRAP1 proteins were mixed as above without addition of nucleotide until the day of SAXS data collection. Once ADP-BeF_3 was added to the reaction 20 μL time points were taken spun down at max speed in a tabletop centrifuge for 10 minutes, and then data was collected. Time points were recorded at the time of exposure.

Data was collected at the ALS at beamline 12.3.1 (Hura et al., 2009) with exposure times of 0.5, 1, and 5 seconds. An additional 2 second exposure was used for the aforementioned time course. Each sample collected was subsequently buffer subtracted and time points were averaged using scripts at beamline 12.3.1 (ogreNew) and in-house software. The scattering data was transformed to P(r) using the program GNOM (Svergun, 1992) and Dmax was optimized. To assess the nature of the closed state the resulting distributions were fit using an in-house least squares fitting program in the region where non-zero data was present for the target data and each model tested. Fitting was done with P(r) curves as previous Hsp90 work indicated they were more effective at discriminating between the models than by comparing I(Q) (Krukenberg et al.,

2008). More specifically, structural differences that are localized in P(r) space tend to be distributed throughout the I(q) data and because of the log scale can be less obvious.

For the fitting we chose to test a combination of a theoretical P(r) curve for each closed state in question and the respective apo data for each reaction. Theoretical scattering curves were generated for each model PDB in the program CRYSOL and transformed with GNOM (Svergun D.I., 1995). The resulting normalized target data and model fit are quantitated using an R-factor that is similar to a crystallography R-factor in nature. R is defined as the equation below:

$$R = \sum |P_{obs}(r) - P_{calc}(r)| / |P_{obs}(r)|$$

where $P_{obs}(r)$ is the observed probability distribution and $P_{calc}(r)$ is the calculated modeled fit.

Apo state data was used for fitting as the equilibrium of states in apo conditions for Hsp90 varies with homolog and condition (Southworth and Agard, 2008). As such, a model for the apo state is a less accurate representation of the apo state and resulted in less optimal fits (judged by R value defined above). Importantly, fitting with either model or data for apo resulted in the same trend of fits, with the asymmetric state giving the best fit. For a comparison, the fits were transformed back into I(q) space an in-house script and displayed in Figure S1B.

The I(q) curves were calculated from fits in P(r) using:

$$I(q) = \Sigma P(r)\sin(qr)/(qr)$$

Residuals were calculated using either of the equations below:

$$\text{Residuals} = P_{calc}(r) - P_{obs}(r) \; ; \quad = I_{calc}(q) - I_{obs}(q)$$

DEER Spectroscopy

Native cysteine residues were replaced in the mature form of human TRAP1 (vector description above) based on conservation with TRAP1 homologs (C261S, C527A, C573R). Two residue positions (within one protomer) were chosen computationally based on solvent accessibility, as well as for optimal resolution between the theoretical distances of asymmetric protomer conformations. Chosen positions (K439 and D684) were replaced with cysteine residues using standard PCR methods to allow for site specific labeling with maleimide functionalized MSL (Sigma). Distance simulations were performed on our closed state model at cryogenic temperatures using rotameric modeling of MTSL labels (MSL not available) at the chosen residue positions using the latest version of multiscale modeling of macromolecular systems, MMM2013 (Polyhach et al., 2011).

Cysteine-free hTRAP1 and cysteine variant for double electron-electron resonance measurements (DEER) were purified as described above with a size exclusion buffer of 20 mM Sodium Phosphate pH 7, 50 mM KCl, 2 mM $MgCl_2$

degassed by purging with N_2 gas to protect cysteine residues of the DEER probe construct. Following size exclusion chromatography, DEER probe protein was labeled ON at 4 °C with a 2:1 excess of MSL:cysteine residue. Excess label was removed by extensive dialysis in size exclusion buffer and labeling was confirmed by CW EPR as in Naber et al (Figure S2A) (Naber et al., 2007).

Cysteine-free and DEER probe protein were then exchanged into a D_2O version of the size exclusion buffer by concentration/dilution in Centricon concentrators (10,000 mwco, Millipore) until the concentration of H_2O was <1%. Unlabeled and labeled proteins were mixed in a 10:1 ratio in apo conditions (final concentration of 30 μM labeled protein) and exchanged at 30 °C for 30 minutes. Reactions were incubated with addition of 2 mM ADP-BeF at 30 °C for 10 hours (as in SAXS) followed by addition of 30% deuterated glycerol (Sigma). Four-pulse DEER data were collected using a Bruker ELEXSYS E580 spectrometer at 34 GHz equipped with a SuperQ-FT pulse Q-band system with a 10 W amplifier and a 5 mm EN5107D2 resonator located at the Ohio Advanced EPR laboratory. Samples of ~10 μl were loaded into a 1.1 mm inner diameter quartz capillary tubes and frozen in liquid nitrogen prior to insertion into the pre-cooled resonator set at 80 K. Data were collected with probe $\pi/2$ and π pulse widths of 10 and 20 ηs and a pump π pulse width of 24 ηs with a repetition time of 700-800 μs and 100 shots/point. The frequency of the pump pulse was adjusted to the maximum in the nitroxide field sweep spectrum and the observed pulse was applied 80 MHz upfield from the pump frequency. The DEER evolution time periods were

from 3.6 – 4.3 μs. T_1 and T_2 values were ~400 μs and ~4.7 μs, respectively. Data were processed and analyzed using DEERAnalysis2013 (Jeschke, 2012) and distance distributions P(r) were obtained from Tikhonov regularization (Chiang et al., 2005), incorporating the constraint $P(r) > 0$. The regularization parameter was optimized to fit the time-domain data without overfitting. The distance distribution data was normalized with an integral of 0.01.

Anisotropy binding measurements

80 μM (dimer concentration) WT hTRAP1 or E551A/L507K MD:CTD interface mutants were pre-closed with 2 mM AMPPNP at 40 °C for 3.5 hours to induce closure. Buffer conditions were 20 mM Hepes pH 7.5, 50 mM KCl, 2 mM $MgCl_2$, and 1 mM DTT with addition of .05% Tween-20 added just prior to binding measurements. Following this, steady-state anisotropy measurements with 600nM IAEDANS-labeled Δ131Δ with WT or mutants were titrated (maintaining AMPPNP concentration) to obtain the affinity for the model substrate. Anisotropy measurements were done as in Street et. al. (Street et al., 2011) with 340 nm excitation and 480 nm emission wavelengths, 5 nM/7 nm (Ex/Em) slit widths, 3 second integration time, at 23 °C.

References:

Adams, P.D., Afonine, P.V., Bunkoczi, G., Chen, V.B., Davis, I.W., Echols, N., Headd, J.J., Hung, L.W., Kapral, G.J., Grosse-Kunstleve, R.W.*, et al.* PHENIX: a comprehensive Python-based system for macromolecular structure solution. Acta Crystallogr D Biol Crystallogr *66*, 213-221.

Chiang, Y.W., Borbat, P.P., and Freed, J.H. (2005). Maximum entropy: a complement to Tikhonov regularization for determination of pair distance distributions by pulsed ESR. J Magn Reson *177*, 184-196.

Cunningham, C.N., Krukenberg, K.A., and Agard, D.A. (2008). Intra- and intermonomer interactions are required to synergistically facilitate ATP hydrolysis in Hsp90. J Biol Chem *283*, 21170-21178.

Doublie, S. (1997). Preparation of selenomethionyl proteins for phase determination. Methods Enzymol *276*, 523-530.

Emsley, P., and Cowtan, K. (2004). Coot: model-building tools for molecular graphics. Acta Crystallogr D Biol Crystallogr *60*, 2126-2132.

Genest, O., Reidy, M., Street, T.O., Hoskins, J.R., Camberg, J.L., Agard, D.A., Masison, D.C., and Wickner, S. (2013). Uncovering a region of heat shock protein 90 important for client binding in E. coli and chaperone function in yeast. Mol Cell *49*, 464-473.

Gill, S.C., and von Hippel, P.H. (1989). Calculation of protein extinction coefficients from amino acid sequence data. Anal Biochem *182*, 319-326.

Gillespie, J.R., and Shortle, D. (1997). Characterization of long-range structure in the denatured state of staphylococcal nuclease. I. Paramagnetic relaxation enhancement by nitroxide spin labels. J Mol Biol *268*, 158-169.

Hura, G.L., Menon, A.L., Hammel, M., Rambo, R.P., Poole, F.L., 2nd, Tsutakawa, S.E., Jenney, F.E., Jr., Classen, S., Frankel, K.A., Hopkins, R.C.*, et al.* (2009). Robust, high-throughput solution structural analyses by small angle X-ray scattering (SAXS). Nat Methods *6*, 606-612.

Jeschke, G. (2012). DEER distance measurements on proteins. Annu Rev Phys Chem *63*, 419-446.

Krukenberg, K.A., Forster, F., Rice, L.M., Sali, A., and Agard, D.A. (2008). Multiple conformations of E. coli Hsp90 in solution: insights into the conformational dynamics of Hsp90. Structure *16*, 755-765.

Leskovar, A., Wegele, H., Werbeck, N.D., Buchner, J., and Reinstein, J. (2008). The ATPase cycle of the mitochondrial Hsp90 analog Trap1. J Biol Chem *283*, 11677-11688.

Ludtke, S.J., Baldwin, P.R., and Chiu, W. (1999). EMAN: semiautomated software for high-resolution single-particle reconstructions. J Struct Biol *128*, 82-97.

Naber, N., Purcell, T.J., Pate, E., and Cooke, R. (2007). Dynamics of the nucleotide pocket of myosin measured by spin-labeled nucleotides. Biophys J *92*, 172-184.

Otwinowski, Z., and Minor, W. (1997). Processing of X-ray diffraction data collected in oscillation mode. Macromolecular Crystallography, Pt A *276*, 307-326.

Pettersen, E.F., Goddard, T.D., Huang, C.C., Couch, G.S., Greenblatt, D.M., Meng, E.C., and Ferrin, T.E. (2004). UCSF Chimera--a visualization system for exploratory research and analysis. J Comput Chem *25*, 1605-1612.

Polyhach, Y., Bordignon, E., and Jeschke, G. (2011). Rotamer libraries of spin labelled cysteines for protein studies. Phys Chem Chem Phys *13*, 2356-2366.

R Development Core Team (2010). R: A language and environment for statistical computing (Vienna, Austria: R Foundation for Statistical Computing).

Schrödinger, L. (2010). The PyMOL Molecular Graphics System.

Southworth, D.R., and Agard, D.A. (2008). Species-dependent ensembles of conserved conformational states define the Hsp90 chaperone ATPase cycle. Mol Cell *32*, 631-640.

Street, T.O., Lavery, L.A., and Agard, D.A. (2011). Substrate binding drives large-scale conformational changes in the Hsp90 molecular chaperone. Molecular cell *42*, 96-105.

Svergun, D. (1992). Determination of the regularization parameter in indirect-transform methods using perceptual criteria. J Appl Crystallogr, 495-503.

Svergun D.I., B.C.a.K.M.H.J. (1995). CRYSOL - a Program to Evaluate X-ray Solution Scattering of Biological Macromolecules from Atomic Coordinates. J Appl Crystallogr, 768-773.